JOURNAL OF MATERIALS SCIENCE 21 (1986) 83–89

# Characterization and thermal behaviour of gel-grown gadolinium tartrate crystals

P. N. KOTRU, N. K. GUPTA, K. K. RAINA, I. B. SHARMA*
*Department of Physics, University of Jammu, Jammu 180001, India*

Gadolinium tartrate crystals in the form of spherulites were synthesized by using a controlled diffusion system in silica gel. Characterization of the material was performed by utilizing the techniques of chemical analysis, X-ray and electron diffraction, infrared and mass spectroscopy, and by its thermal behaviour. The material turns out to be a dihydrate and the chemical composition was thus established as $Gd_2(C_4H_4O_6)_3 \cdot 2H_2O$. The data obtained from the thermal analysis show the tendency of the material to decompose, and this is further confirmed by mass spectroscopy. The decomposition process is completed in four steps until gadolinium oxide is obtained at 840° C. The energetics of the reactions at each stage of decomposition have been examined and mechanisms for the decomposition reactions are proposed.

## 1. Introduction

Considerable interest now exists in the properties of materials involving rare-earth ions, on account of their optical and magnetic properties. The present work concerns the characterization of gel-grown gadolinium tartrate spherulitic cyrstals. In the present work, crystals of $Gd_2(C_4H_4O_6)_3 \cdot 2H_2O$ were grown by using a controlled diffusion system of silica gel [1]; typical crystals are shown in Fig. 1. The gadolinium tartrate crystals grown here are different from those reported in the literature [2]. Pastorek and Monatsh [2] reported the material to have five waters of hydration, whilst our work establishes only two. Growth of dihydrated gadolinium tartrate spherulitic crystals by the gel technique has already been reported by Kotru *et al* [1]. The present work reports characterization of the material by chemical analysis, infrared (IR) and mass spectroscopy, X-ray and electron diffraction, and by its thermal behaviour.

## 2. Experimental details

To determine the amount of gadolinium (metal), carbon and hydrogen, the material was subjected to conventional physical and chemical analysis. Carbon–hydrogen analysis was carried out by using carbon–hydrogen analysing equipment. X-ray powder diffraction patterns were obtained using a Philips X-ray powder diffractometer Model PW1350 with nickel-filtered Cu$K\alpha$ radiation (30 kV, 15 mA). The sample was scanned with a scanning speed of 2° in $2\theta$ per minute. The ratemeter and chart speed were kept constant for all the runs. Electron diffraction patterns, mass and IR spectra (400 to 4000 $cm^{-1}$) were recorded by employing AEI TEM–802(UK), JMS–300 mass spectrometer and Spektromom 2000 (using the KBr pellet technique), respectively. The thermal analysis, involving differential thermal and thermogravimetric analyses (DTA, TGA) and DTG techniques, was performed by means of a Paulik–Paulik–Eredey MOM derivatograph (Hungary) at a heating rate of 10° C $min^{-1}$. The weight of the sample for this purpose was taken as 200 mg. For identifying the final product in TGA analysis, an X-ray powder pattern was recorded after heating the original compound to 840° C in an electronically controlled muffle furnace working within an accuracy of ± 10° C. The energetics and order of reactions were calculated using different thermodynamic equations as described at the relevant places in the text.

## 3. Results and discussion

### 3.1. Chemical analysis

The composition of gadolinium tartrate was established using metal and carbon–hydrogen analysis. The results of the analysis, given in Table I, suggest the material to be a dihydrate. The composition of the material is thus established as $Gd_2(C_4H_4O_6)_3 \cdot 2H_2O$. The dihydration of the material is further supported by the thermogram (TG) (the details of which follow in the text), where, after a mass loss of 55%, $Gd_2O_3$ is formed. Knowing the initial mass of the sample and the subsequent mass loss, the calculations carried out for $Gd_2(C_4H_4O_6)_3 \cdot 2H_2O$ completely agree with those obtained from the chemical analysis.

### 3.2. X-ray analysis

The X-ray diffractogram recorded on the material, as shown in Fig. 2, indicates crystallinity of the sample. The X-ray diffraction data are given in Table II. To the best of the authors' knowledge, the data reported here are entirely new. It is interesting to note here that the X-ray powder data available in the literature [2] report the existence of gadolinium tartrate, with five waters of hydration. The difference in the X-ray

*Present address*: Department of Chemistry, University of Jammu, Jammu 180001, India.

0022–2461/86 $03.00 + .12 © *1986 Chapman and Hall Ltd.*

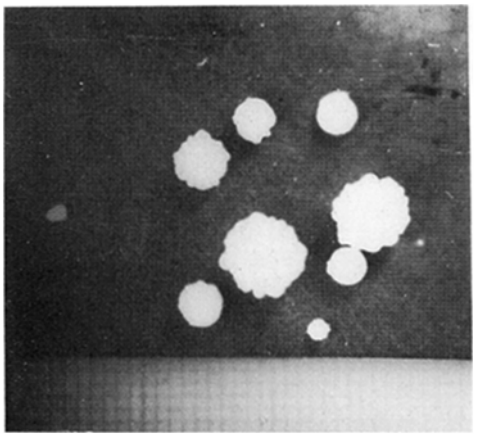

*Figure 1* Gel-grown spherulitic crystals of dihydrated gadolinium tartrate (1 mm grid).

powder data in the two cases is thus expected, considering the difference of waters of hydration. The X-ray powder pattern of the final product in TGA (after the sample is heated to 840° C and the mass loss is constant) has a striking resemblance with the existing data available for $Gd_2O_3$ [3]. Here the prediction of the final product being $Gd_2O_3$ finds confirmation.

### 3.3. Transmission electron microscopy

Fig. 3 shows the electron diffraction patterns of the material recorded immediately on and after some time of loading. Fig. 3a shows a spotty diffraction pattern indicating crystallinity of the material. Comparison of

TABLE I Chemical analysis of $Gd_2(C_4H_4O_6)_3 \cdot 2H_2O$ (MW = 794.5)

| Element | Composition (%) | |
|---|---|---|
| | Theoretical | Measured |
| Gd | 39.5 | 37.15 |
| C | 18.13 | 16.5 |
| H | 2.01 | 3.0 |

Figs. 3a and b reveals a change in the state of crystallinity during examination of the sample in the transmission electron microscope, indicating decomposition of the material; the diffraction pattern suggests a change from some polycrystallinity to further polycrystallinity [4]. This transition in the diffraction pattern is also attributed to the presence of water of hydration in the original material. Materials with water of hydration pose such problems on being examined with an electron microscope [5], which limits the scope of this technique for their in-depth study. Because of the immediate decomposition of the material, it is not possible to state categorically whether the diffraction pattern recorded immediately on loading is that of the parent material or not.

### 3.4. Mass spectroscopy

The mass spectrum of the sample was recorded using 70 eV electron bombardment for ionization. The mass spectrum suggests decomposition of the material and further supports the presence of water, carbon and

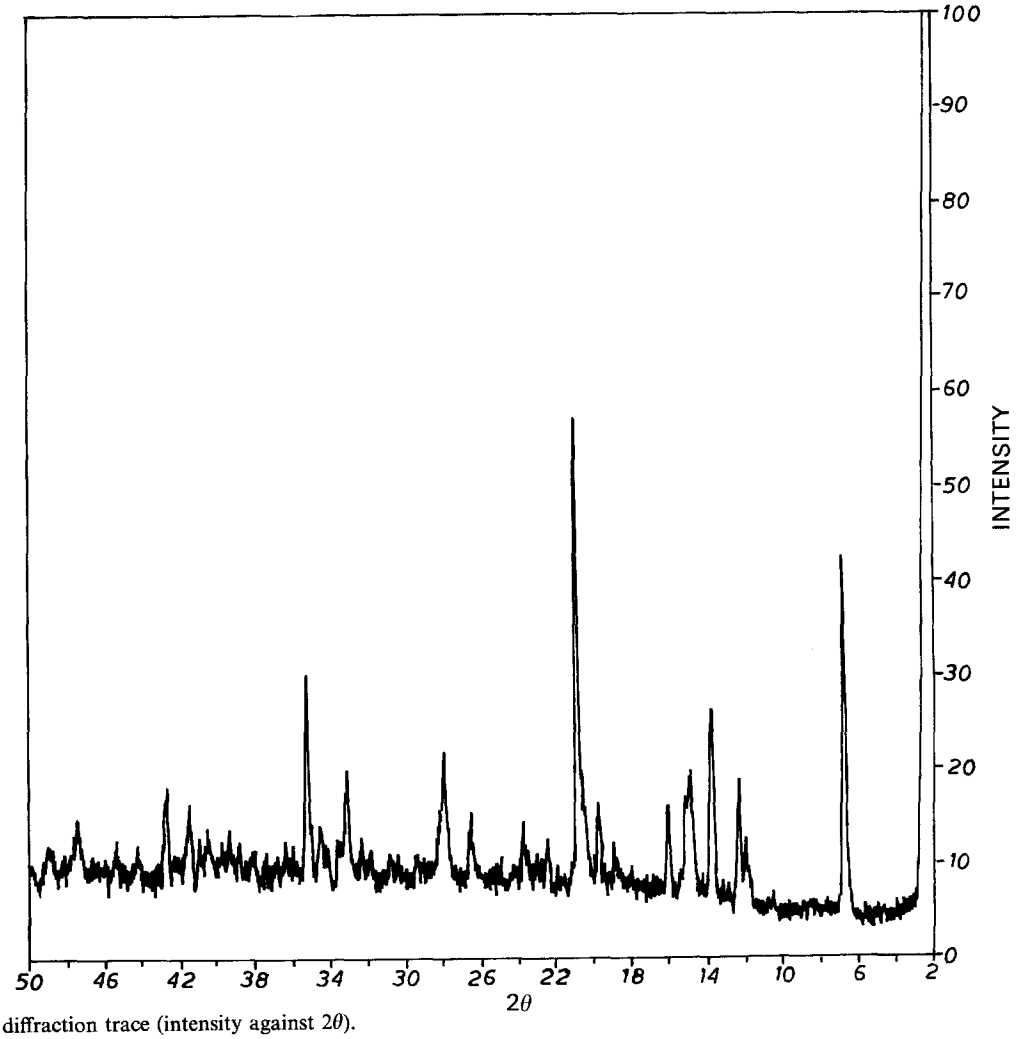


*Figure 2* X-ray diffraction trace (intensity against $2\theta$).

TABLE II X-ray powder data

| $d$(nm) | Intensity values |
|---|---|
| 1.3392 | 39 |
| 0.73750 | 14 |
| 0.64634 | 20.5 |
| 0.59454 | 14 |
| 0.55049 | 9.5 |
| 0.44838 | 8.5 |
| 0.41907 | 49.5 |
| 0.33634 | 7.5 |
| 0.31865 | 14 |
| 0.26905 | 12.5 |
| 0.25286 | 22 |
| 0.21175 | 10.5 |

oxygen as its constituents, as is expected on fragmentation of the tartrate and water of crystallization in the parent material. Repeated experiments performed in an attempt to capture the molecular ion along with the metal, had there been some volatility, failed to yield the desired results. Since we failed to get the molecular ion, it is clearly indicated that the molecule decomposes before it is captured. Fig. 4 shows the mass spectrum obtained for $Gd_2(C_4H_4O_6)_3 \cdot 2H_2O$. The mass fragmentography is suggested by Table III. The base-peak of $M/E = 18$ (Table III) indicates the possible presence of water of crystallization. The $M/E$ peak at 149 is suggested to be due to the tartrate constituent of the parent material, the molecule being

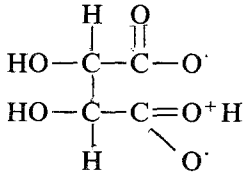

The mass spectrometry supplements the findings from chemical analysis, IR and TGA regarding the chemical composition, besides suggesting the fragmentography at 70 eV by electron bombardment and decomposition of the parent material.

## 3.5. IR spectroscopy

Fig. 5 shows the infrared spectrum recorded for $Gd_2(C_4H_4O_6)_3 \cdot 2H_2O$. The results obtained from the IR spectrum are summarized in Table IV. The band assignment made here attributes the peak at 3040 $cm^{-1}$ to strongly stretching interactions of OH

TABLE III Mass spectrum data of $Gd_2(C_4H_4O_6)_3 \cdot 2H_2O$

| $M/E$ | Raw intensity | Normalized intensity | Σ(%) |
|---|---|---|---|
| 1.0 | 1.6 | 1.6 | 0.09 |
| 14.0 | 6.4 | 6.4 | 0.36 |
| 16.0 | 11.6 | 11.6 | 0.65 |
| 17.0 | 209.4 | 210.6 | 11.84 |
| 18.0 | 994.6 | 1000.0 | 56.22 |
| 19.0 | 14.2 | 14.3 | 0.80 |
| 20.0 | 2.3 | 2.3 | 0.13 |
| 27.0 | 1.4 | 1.4 | 0.07 |
| 28.0 | 355.2 | 357.1 | 20.08 |
| 29.0 | 6.2 | 6.2 | 0.35 |
| 30.0 | 0.9 | 0.9 | 0.05 |
| 32.0 | 83.6 | 84.1 | 4.72 |
| 39.0 | 1.2 | 1.2 | 0.07 |
| 40.0 | 6.3 | 6.3 | 0.35 |
| 41.0 | 3.5 | 3.5 | 0.20 |
| 42.0 | 0.9 | 0.9 | 0.05 |
| 43.0 | 5.0 | 5.0 | 0.28 |
| 44.0 | 12.2 | 12.3 | 0.69 |
| 45.0 | 0.9 | 0.9 | 0.05 |
| 55.0 | 3.3 | 3.3 | 0.18 |
| 56.0 | 1.1 | 1.1 | 0.06 |
| 57.0 | 4.9 | 4.9 | 0.27 |
| 67.0 | 1.2 | 1.2 | 0.07 |
| 69.0 | 2.9 | 2.9 | 0.16 |
| 70.0 | 1.2 | 1.2 | 0.07 |
| 71.0 | 3.0 | 3.0 | 0.17 |
| 79.0 | 1.0 | 1.0 | 0.05 |
| 81.0 | 1.8 | 1.8 | 0.10 |
| 83.0 | 1.6 | 1.6 | 0.09 |
| 85.0 | 1.3 | 1.3 | 0.07 |
| 91.0 | 1.5 | 1.5 | 0.08 |
| 93.0 | 1.5 | 1.5 | 0.08 |
| 95.0 | 2.2 | 2.2 | 0.12 |
| 97.0 | 1.1 | 1.1 | 0.06 |
| 105.0 | 1.4 | 1.4 | 0.07 |
| 107.0 | 1.1 | 1.1 | 0.06 |
| 109.0 | 2.5 | 2.5 | 0.14 |
| 110.0 | 1.4 | 1.4 | 0.08 |
| 113.0 | 1.2 | 1.2 | 0.06 |
| 119.0 | 1.2 | 1.2 | 0.07 |
| 121.0 | 1.3 | 1.3 | 0.07 |
| 135.0 | 0.9 | 0.9 | 0.05 |
| 136.0 | 1.2 | 1.2 | 0.07 |
| 149.0 | 4.1 | 4.1 | 0.23 |
| 189.0 | 1.1 | 1.1 | 0.06 |
| 205.0 | 1.4 | 1.4 | 0.08 |
| 218 | 1.0 | 1.0 | 0.06 |

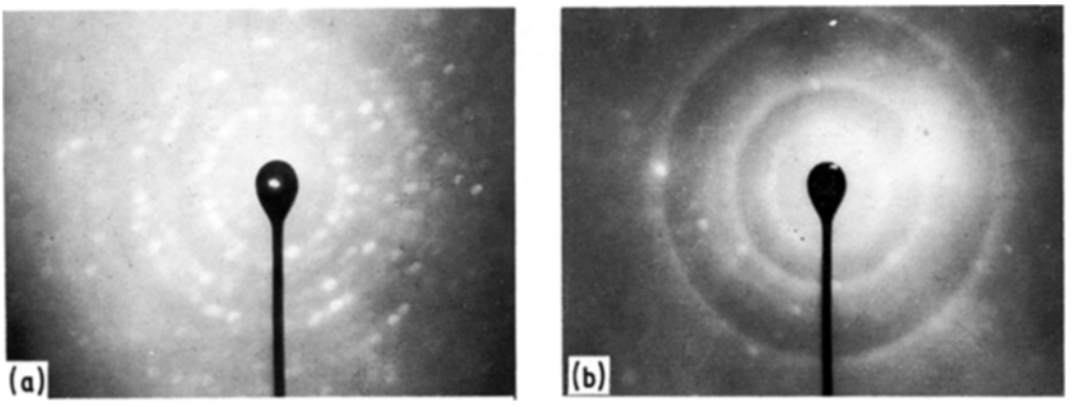


*Figure 3* (a) Transmitted electron diffraction pattern recorded immediately on loading; (b) diffraction pattern recorded after some time of loading.

TABLE IV Infrared band assignment for $Gd_2(C_4H_4O_6)_3 \cdot 2H_2O$

| Band ($cm^{-1}$) | Assignment |
|---|---|
| 3040 (strong) | Water (strongly stretching vibration of OH group) |
| 1570 (weak), 1530 (weak) | C=O vibration |
| 1400 (strong), 1310 (strong) | CO symmetrical + $\delta$O—C = O |
| 1125 (strong), 1070 (strong) | $\delta$CH and $\pi$CH |

groups. In the formation of carboxylate ions the frequencies of the carboxyl group of the acid and its C–O vibration get merged, and the resultant twin peaks are formed at 1570 and 1530 $cm^{-1}$. The peaks at 1400 and 1310 $cm^{-1}$ are due to symmetrical C–O vibrations of the carboxylate anion. The peaks at 1125 $cm^{-1}$ and 1070 $cm^{-1}$ correspond to $\delta$CH and $\pi$CH vibrations. The infrared spectrum reveals that the product obtained in the gel-growth system [1] yield a well-defined salt, established as $Gd_2(C_4H_4O_6)_3 \cdot 2H_2O$.

## 3.6. Thermal analysis

The thermograms showing TG and DTA, DTG recorded for $Gd_2(C_4H_4O_6)_3 \cdot 2H_2O$ are shown in Figs. 6 and 7 respectively. The TG curve shows that the material starts decomposing at about 50° C and the process gets completed after the mass loss attains saturation. The process of decomposition involves four distinct stages. In the first stage between 50 and 170° C, 7% of the mass is lost which corresponds to three water molecules (including two molecules of water of hydration). In the second stage between 170 and 275° C, the mass loss of 4.7% results in the elimination of two more water molecules. The third and fourth stages are completed at 380 and 840° C respectively, the accompanying mass losses being 17 and 25%. Table V gives a summarized analysis of the different stages associated with the thermal decomposition of the material as observed in the thermogram (TG) of Fig. 6. From the mass-loss calculations the stoichiometry of the decomposition reactions is proposed, as detailed in Fig. 8.

To further understand the reaction kinetics, the equations of Horowitz and Metzger [6], Piloyan and Novikova [7] and Coats and Redfern [8] were used in calculating the activation energy $E$ at different stages of decomposition. The order of reaction for all the four stages in the TGA was calculated using the Horowitz–Metzger relation. The equations used are given below.

TABLE V Results of decomposition process of $Gd_2(C_4H_4O_6)_3 \cdot 2H_2O$

| Stage | Temperature range (° C) | Observed mass loss (%) | Calculated mass loss (%) | Loss of molecules in the step |
|---|---|---|---|---|
| I | 50 to 170 | 7 | 6.79 | $3H_2O$ |
| II | 175 to 275 | 4.5 | 4.53 | $2H_2O$ |
| III | 275 to 380 | 15.5 | 15.86 | $3H_2O$ and 6CO |
| IV | 380 to 840 | 28 | 27.18 | $6CO_2$ |

### 3.6.1. Horowitz–Metzger relation

$$\log\left(\frac{1-(1-\alpha)^{1-n}}{1-n}\right) = \frac{E\theta}{2.303RT_m^2}$$

where $T - T_m = \theta$, provided $n \neq 1$: i.e. $n = 1/2$, 1/4, 2/3, 1/3 . . . ; $\alpha$ = weight loss upto a particular temperature divided by total weight loss in the step, $n$ is the order of reaction and $R$ is the gas constant. $T_m$ can be obtained as a function of $\alpha$ and $T$, where $T$ is temperature at a particular place. A plot of the LHS of the equation against $\theta$ shows a linear dependence, from the slope of which the energy of activation can be calculated.

### 3.6.2. Piloyan–Novikova relation

$$\log \alpha/T^2 = \log(ZR/\beta E) - E/2.303\,RT$$

where $\alpha$ = 0.05 to 0.5; $\alpha$ = weight loss up to a particular temperature divided by total weight loss in the step, $\beta$ = rate of increase of temperature, $T$ = absolute temperature, $Z$ is a frequency factor, $E$ can be calculated by plotting $\log \alpha/T^2$ against $1/T$ and $Z$ from the intercept of the graph obtained.

### 3.6.3. Coats–Redfern relation

$$\log\frac{\log C^{-1}}{T^2} = \log\frac{ZR}{\phi E} - \frac{E}{2.303\,RT}$$

Here $C = (W_{0c} - W)/W_{0c}$, where $W_{0c}$ = total mass loss for a particular stage, $W$ = mass loss at absolute temperature $T$, $Z$ is a pre-exponential factor and $\phi$ the heating rate. Plotting $\log(\log C^{-1}/T^2)$ against $1/T$ gives the value of the activation energy.

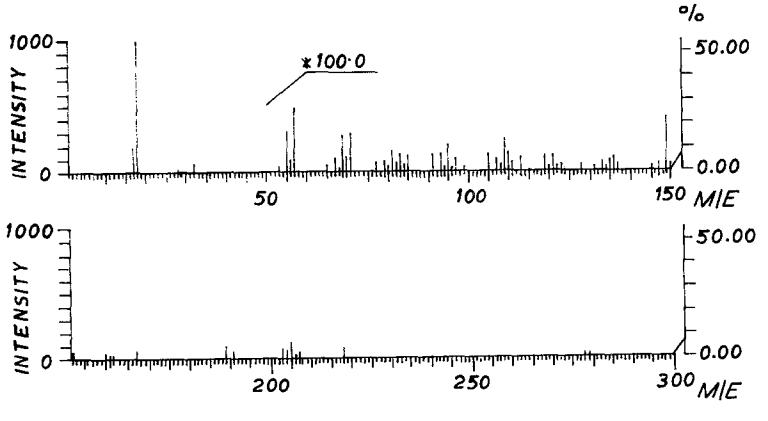


*Figure 4* Mass spectrum.

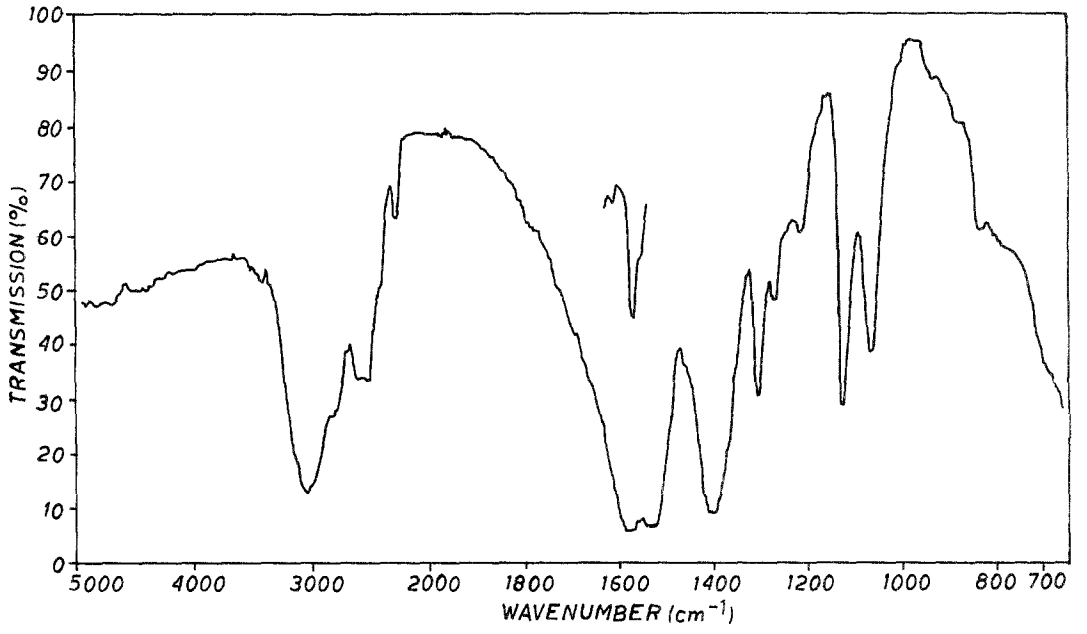


*Figure 5* Infrared spectrum.

### 3.6.4. Analysis of results

Table VI gives the values of activation energy and the order of reaction pertaining to different stages of decomposition in the thermogram (TG), as calculated by using the above equations. The table shows that the values of activation energy at different stages are reasonably consistent with those based on the Horowitz–Metzger (H–M) and Coats–Redfern (C–R) relations. There are, however, deviations from such values when calculations are based on the Piloyan–Novikova (P–N) relation.

Fig. 7, showing the differential thermal behaviour of $Gd_2(C_4H_4O_6)_3 \cdot 2H_2O$, exhibits three endothermic peaks corresponding to the first three steps in the TG and two exothermic peaks corresponding to the last TG step. From this, it is indicated that the last TG step is composed of two decomposition processes. However, in the thermogram of Fig. 6 there does not seem to be any clear-cut arrest/separation between the last two exothermic peaks, though they are clearly demarcated in the DTA (Fig. 7), indicating that the species at this stage is unstable. To calculate the activation energy from DTA, the following relation due to Borchardt and Daniels [9] has been used:

$$k = \Delta T/(A - a)$$

where $k$ = specific reaction rate, $\Delta T$ = peak height at any temperature $T$, $A$ = total area of the peak and $a$ = area of the peak at the temperature $T$.

The activation energy values thus calculated are given in Table VII. It is observed from the table that the values of activation energy corresponding to the first three steps are in reasonably good agreement with the values obtained from the thermogram (Table VI) using the H–M and C–R relations. However, there is a disagreement with the values obtained by using the P–N relation. Comparison of the last two values from DTA (Table VII) with the one got from TGA (Table VI) is not of much significance, as the contribution from each DTA step to the overall reaction indicated by TGA is not understood.

The low values of energy of activation indicate that the rate of reaction may be controlled by nucleation processes.

## 4. Conclusions

1. The gel-grown system, involving the use of gadolinium chloride or gadolinium nitrate as the upper reactant and a sodium metasilicate gel impregnated with tartaric acid [1], yields a well-defined salt of gadolinium tartrate which crystallizes in the form of spherulites.

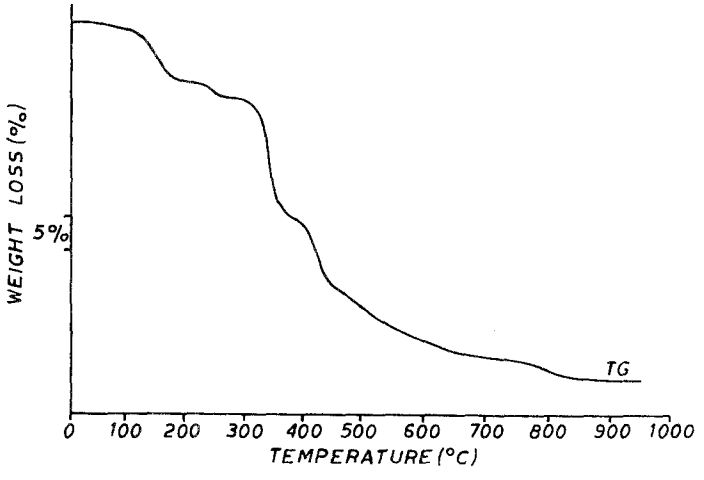


*Figure 6* TG curves for gadolinium tartrate crystals of composition $Gd_2(C_4H_4O_6)_3 \cdot 2H_2O$.

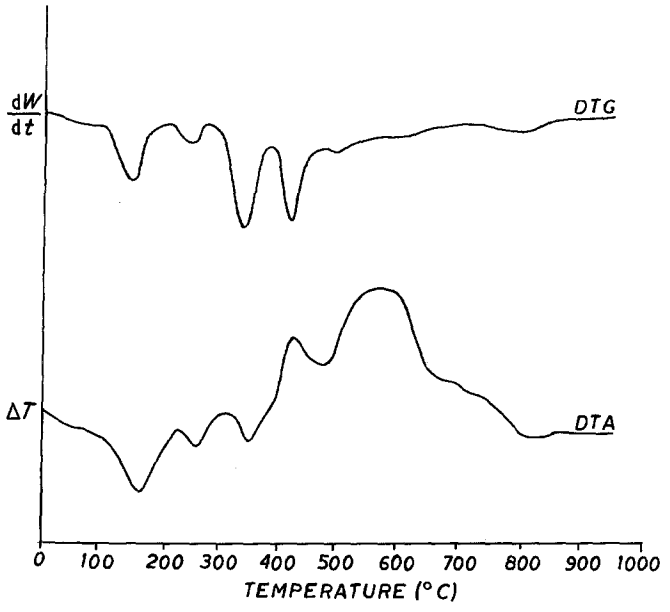


*Figure 7* Thermal analysis (DTG and DTA) curves for gadolinium tartrate crystals of composition $Gd_2(C_4H_4O_6)_3 \cdot 2H_2O$.

2. X-ray and electron diffraction data reveal crystallinity of the gel-grown gadolinium tartrate spherulites.

3. Chemical analysis coupled with the findings from infrared spectroscopy and TGA establish the composition of the material to be $Gd_2(C_4H_4O_6)_3 \cdot 2H_2O$. The X-ray data recorded are different from those reported [2] for $Gd_2(C_4H_4O_6)_3 \cdot 5H_2O$, which establishes the material grown here to have a different stoichiometry from the one already known.

4. The results of mass spectroscopy and thermal analysis (DTA, DTG and TGA) suggest the material to be thermally unstable even at lower energies, the decomposition of the material having been observed at an energy of 70 eV in the case of mass spectroscopy. Changes in the electron diffraction pattern recorded

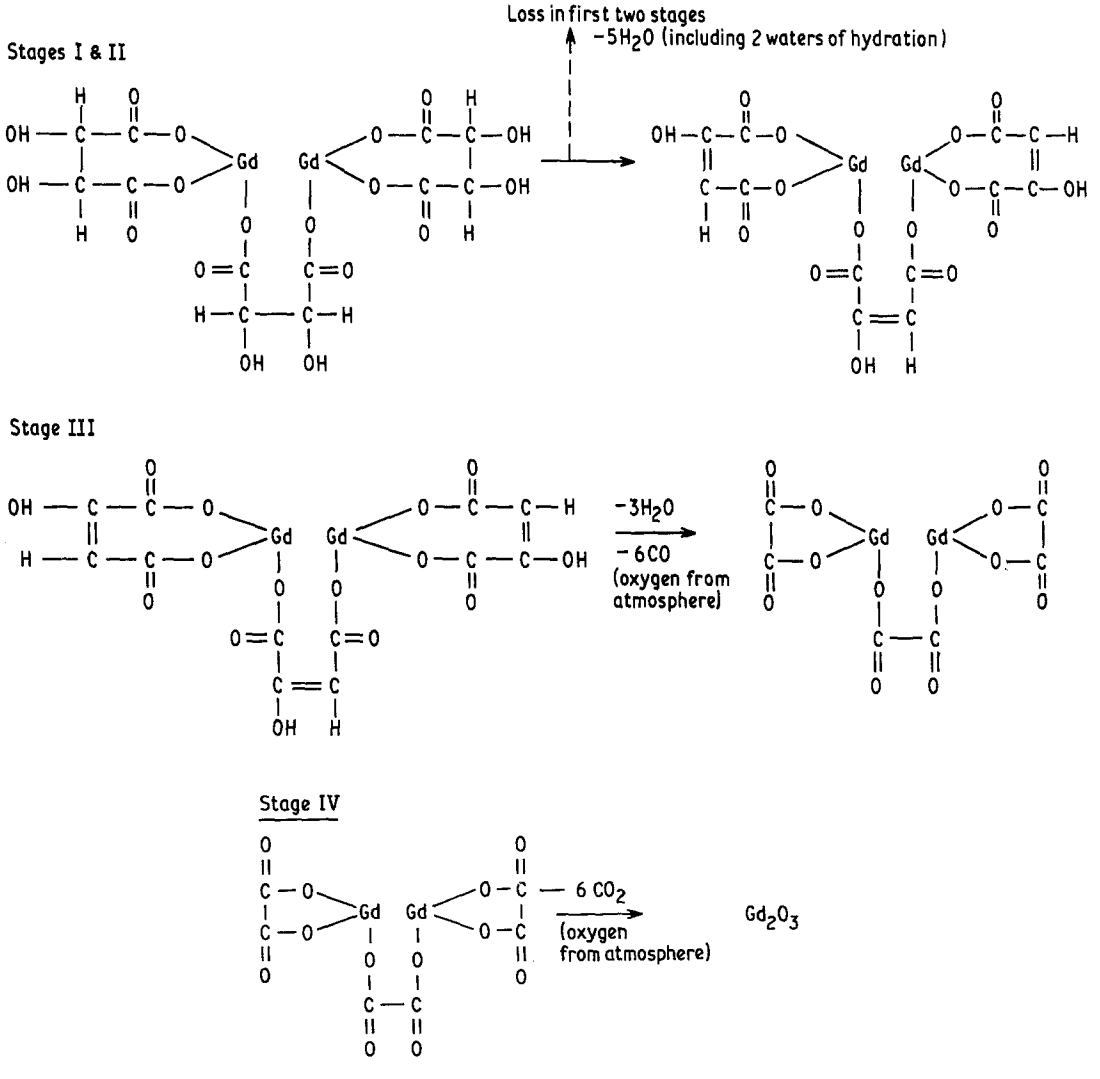


*Figure 8* Stages of decomposition reactions.

TABLE VI Energy of activation and order of reaction

| Relation used | Stage | Order of reaction $n$ | Activation energy $E_a$ (kcal mol$^{-1}$)* |
|---|---|---|---|
| Horowitz–Mertzger [6] | I | 0.5 | 13.981 |
| | II | 0.5 | 20.944 |
| | III | 0.75 | 26.237 |
| | IV | 0.75 | 35.86 |
| Piloyan–Novikova [7] | I | – | 6.971 |
| | II | – | 7.628 |
| | III | – | 8.5 |
| | IV | – | 7.168 |
| Coats–Redfern [8] | I | – | 13 |
| | II | – | 28 |
| | III | – | 18 |
| | IV | – | 49 |

*1 kcal = 4.187 KJ.

immediately on and after some time of loading reveal changes in the state of crystallinity due to electron beam heating and the presence of water of hydration in the material.

5. The thermal behaviour of the material reveals that its decomposition starts at 50° C and, after four stages of decomposition, it gets reduced to $Gd_2O_3$ at 840° C. The activation energy of reaction calculated at different steps of decomposition, using the Horowitz–Metzger, Coats–Redfern and Piloyan–Novikova relations, range from 6 to 49 kcal mol$^{-1}$ (25 to 205 kJ mol$^{-1}$). Energies of such an order suggests that the rate of reaction may be controlled by nucleation processes. The order of reaction as estimated by using the H–M equation in the TGA is 0.5 for the first two steps of decomposition and 0.75 for the remaining two steps of decomposition.

## Acknowledgements

The authors are grateful to the University Grants Commission for a teacher fellowship (N.K.G.) and to the University authorities for a research fellowship (K.K.R.). They also thank Dr M. L. Koul, Department of Chemistry, University of Jammu for his valuable suggestions. One of us (P.N.K.) is grateful to the UGC. for approval of the research project and for the offer of financial assistance.

TABLE VII Energy of activation results from DTA recording

| Relation used | Peak | Activation Energy $E_a$ (kcal mol$^{-1}$)* |
|---|---|---|
| Borchardt and Daniels [9] | 1st | 16 |
| | 2nd | 30 |
| | 3rd | 28 |
| | 4th | 38 |
| | 5th | 28 |

*1 kcal = 4.187 kJ.

## References

1. P. N. KOTRU and N. K. GUPTA, Proceedings of National Seminar on Crystal Growth, 4–6 October, 1982 (Crystal Growth Centre, Anna University, Madras) p. 70.
2. PASTOREK and MONATSH, *Chem.* **101** (1970) 693.
3. GUENTERT and MOZZI, *Acta Crystallogr.* **11** (1958) 746.
4. P. N. KOTRU and N. K. GUPTA, *Bull. Electron Microsc. Soc. Ind.* **7** (1983) 119.
5. M. H. LORENTTO, "Physico-chemical Methods of Mineral Analysis", edited by A. W. Nicol (Plenum Press, New York, 1975) p. 324.
6. H. H. HOROWITZ and G. METZGER, *Anal. Chem.* **35** (1963) 1464.
7. G. O. PILOYAN and O. S. NOVIKOVA, *Russian J. Inorg. Chem.* **12** (1966) 313.
8. A. W. COATS and J. P. REDFERN, *Nature* **201** (1964) 68.
9. H. J. BORCHARDT and F. DANIELS, *J. Amer. Chem. Soc.* **79** (1957) 41.

*Received 23 November 1984*
*and accepted 28 February 1985*